Neuron, volume 58

Supplemental Data

Synapse-Specific Adaptations to Inactivity in Hippocampal Circuits Achieve Homeostatic Gain Control While Dampening Network Reverberation

Jimok Kim and Richard W. Tsien

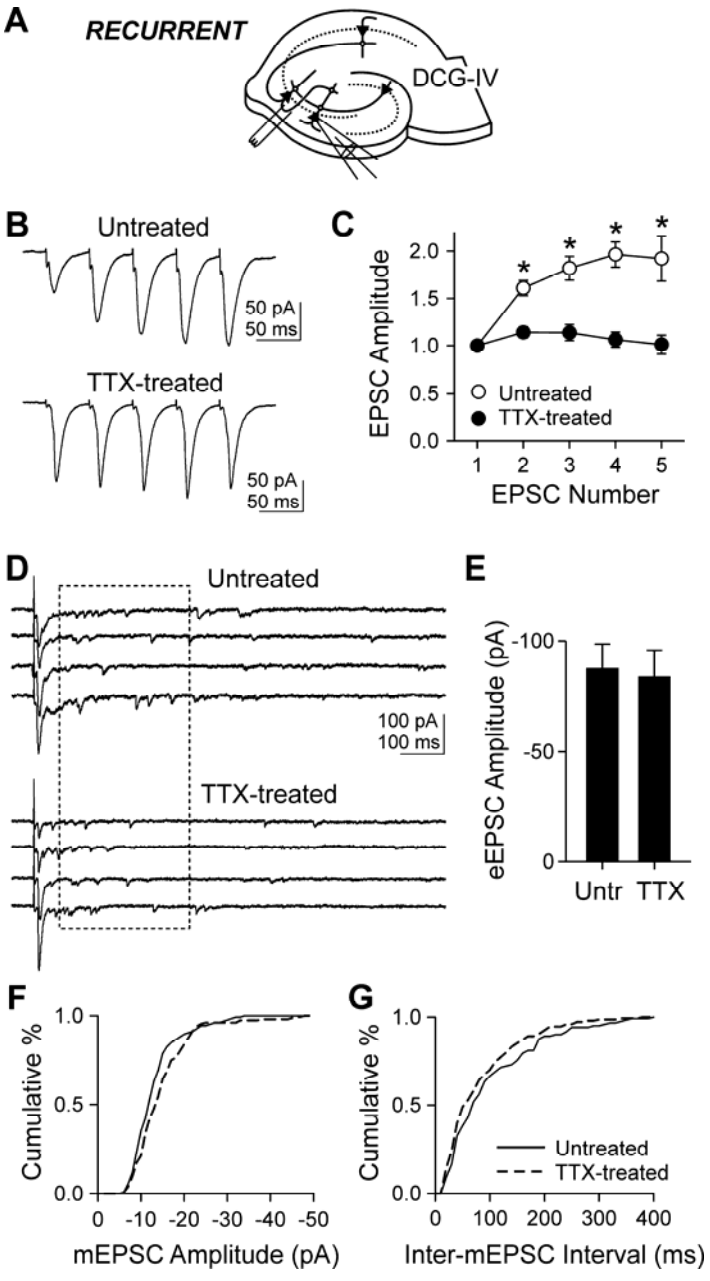

Supplemental Figure 1. Properties of Recurrent Synaptic Transmission

(A) Schematic of recording recurrent synaptic activity. DCG-IV (1 - 2 μM) was present throughout the experiments.

(B) Short-term plasticity at 50 Hz with elevated release probability in 2-chloroadenosine (5 μM). The bath solution was normal saline with addition of 10 μM gabazine, 50 μM D-AP5, 5 μM 2-chloroadenosine, 1 μM DCG-IV and 5 nM TTX.

(C) Group data of short-term plasticity in 2-chloroadenosine (n = 5 for each of untreated and TTX group). Note that facilitation, especially in control condition, is larger than Figure 3C, which was recorded without 2-chloroadenosine. *, $p<0.05$, Bonferroni *t*-test after two-way ANOVA.

(D) EPSCs were evoked when extracellular Ca^{2+} was substituted with 4 mM Sr^{2+}. Evoked asynchronous EPSCs were analyzed in the window of 60 - 360 ms after the stimulation (dashed rectangle). In this experiment, the bath solution contained (in mM) 117 NaCl, 3 KCl, 4 $SrCl_2$, 4 $MgCl_2$, 26 $NaHCO_3$, 1 NaH_2PO_4, 20 glucose, 0.05 D-AP5, 0.002 DCG-IV and 5 nM TTX. The composition of pipette solution was (in mM) 125 $CsCH_3SO_3$, 1 $MgCl_2$, 10 Hepes, 0.4 EGTA, 2 ATP-Mg, 0.3 GTP-tris, 5 QX314-Br and 10 phosphocreatine. Instead of using a $GABA_A$ receptor blocker, cells were held at the reversal potential of IPSC, -63 mV. The IPSC reversal potentials were determined in separate experiments to be -62.5 ± 1.5 mV (n = 7 untreated cells) and -63.9 ± 1.1 mV (n = 8 TTX-treated cells). Two means were not significantly different ($p>0.4$, *t*-test), thus the holding potential in subsequent experiments was set near the grand mean of pooled 15 cells, -63.2 ± 0.91 mV. In a subset of cells (n = 3 each for control and TTX group), EPSC recording was assured by confirming 10 μM NBQX eliminated all detectable synaptic currents, either evoked or spontaneous (data not shown).

(E) Mean amplitude of evoked synchronous EPSC in Sr^{2+} was not different between untreated (n = 5) and TTX-treated (n = 6) slices ($p>0.8$, *t*-test).

(F) Histograms of amplitudes of asynchronous quantal responses in Sr^{2+}. $p>0.02$, K-S test.

(G) Histogram of inter-event interval of asynchronous quantal release shows no difference ($p>0.2$, K-S test). In a given cell, inter-event interval was measured after concatenating individual 300-ms sweeps.

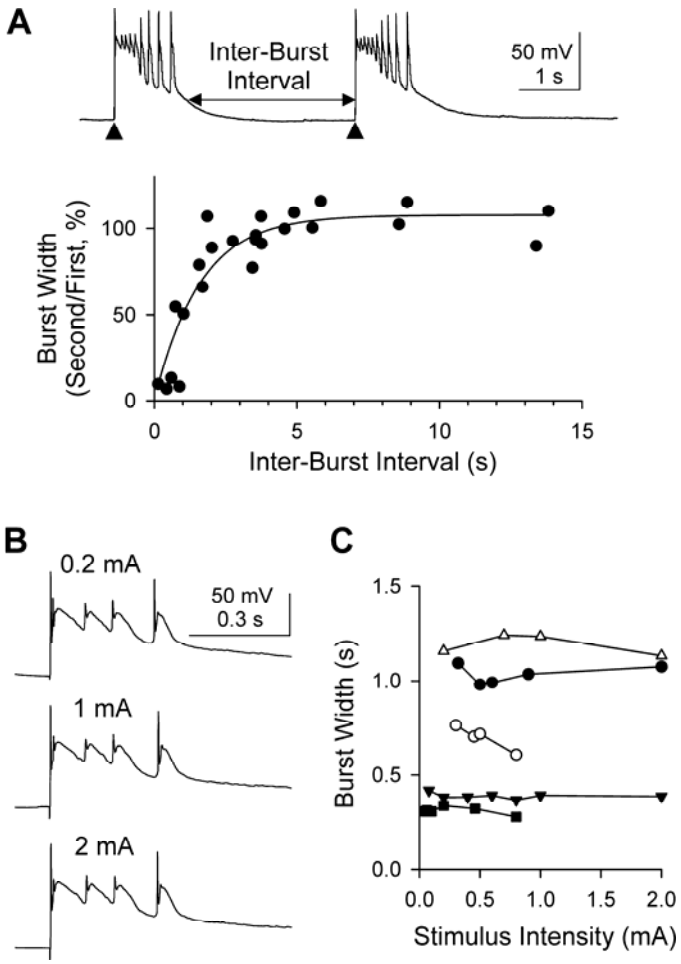

Supplemental Figure 2. Effects of Inter-Burst Interval and Stimulus Intensity on Burst Width
(A) Recovery of burst width with increasing separation from a preceding burst. Two bursts were evoked by stimuli (triangles) delivered at varying intervals by an extracellular stimulating electrode placed at the border of st. oriens and pyramidale. Inter-burst interval was defined as a time between the termination of the first burst (20% of peak plateau amplitude; see Experimental Procedures for details) and the beginning of the second burst (time at the point of maximum rising slope of the first action potential in the burst). The width of the second burst was normalized to the width of the first burst, and the ratio was plotted against the inter-burst interval. Data are from six untreated cells. Each dot represents one trace. The data were fitted with a curve $y = k\,[1 - \exp(-x/\tau)]$, where $\tau = 1.60$ s and correlation coefficient $R^2 = 0.84$.
(B-C) Stimulus intensity had little effect on the burst width.
(B) Recording of bursts from a single cell at three different stimulus intensities indicated.
(C) The burst width was plotted against stimulus intensity. Each symbol represents each cell.

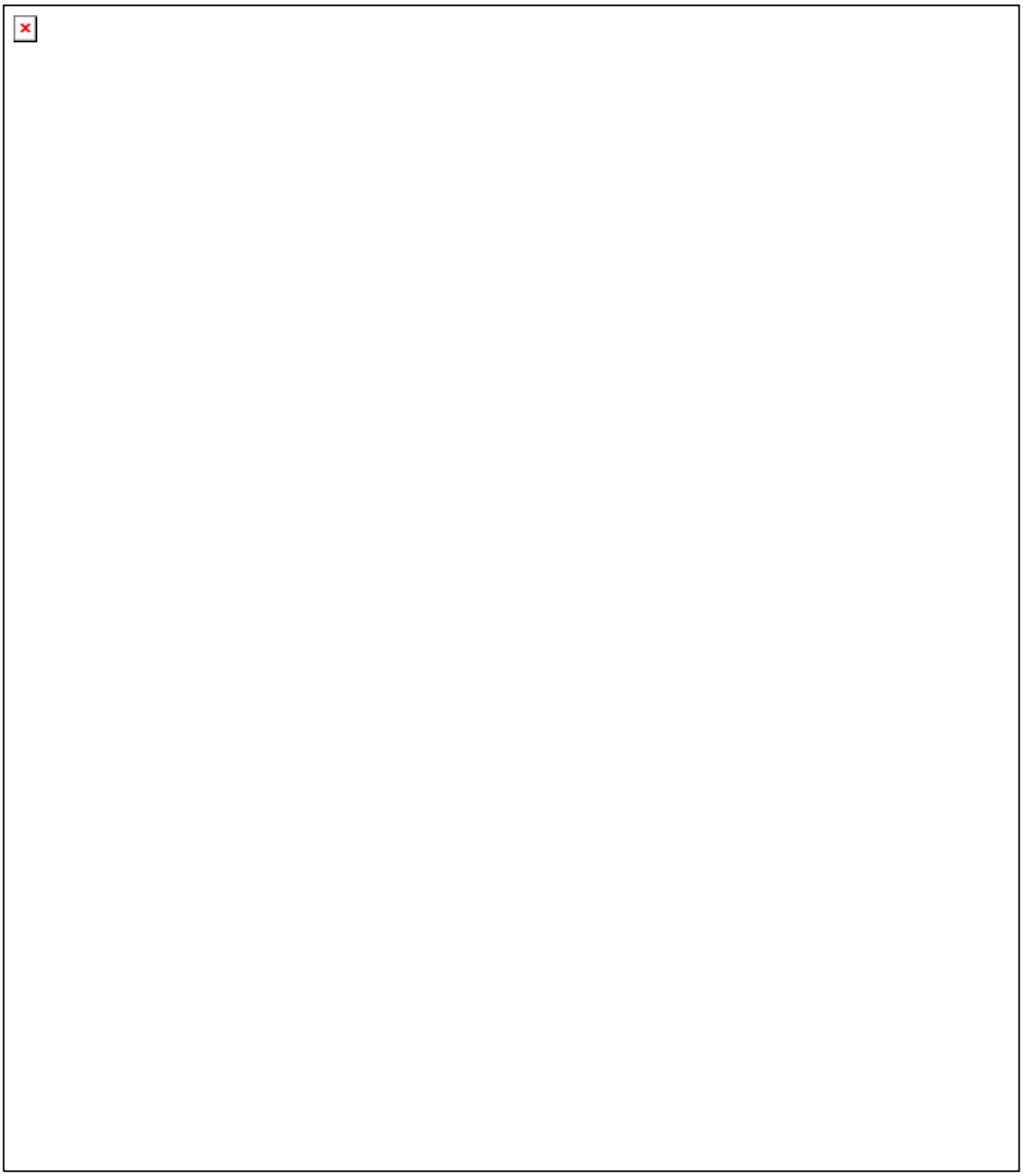

Supplemental Figure 3. Inactivity-Induced Changes in Action Potential Parameters Reflecting Major Ionic Currents Involved in Spike Generation

The predominant voltage-gated Na^+ and K^+ channels are not responsible for regional differences in how repetitive firing properties change with activity deprivation.

(A-C) Analysis of the voltage-response to a single pulse of applied current (in this case, I_{inj} was 200 nA).

(B) Expanded version of the first spike in response to the applied current, with markers of the voltage levels of threshold and peak (filled arrowheads), the times of the threshold crossings in depolarizing and repolarizing directions (t_{dth} and t_{rth}) and the time of the action potential peak (t_{peak}).

(C) Third derivative of the voltage signal, used to determine the threshold point as indicated (Henze and Buzsaki, 2001).

(D-I) Examination of changes in spike features in CA3 pyramidal cells, reflecting principal ionic currents supporting the action potential, which in principle might help govern inter-spike trajectory and repetitive firing (Bean, 2007).

(D-F) Spike features indicative of the strength of inward Na^+ current, which in other systems may be upregulated by chronic inactivity (Aptowicz et al., 2004; Desai et al., 1999).
(D) Action potential threshold.
(E) Action potential peak level.
(F) Maximum depolarizing slope. The significantly slower upstroke in TTX-treated group is qualitatively consistent with the inactivity-induced reduction in excitability of CA3 pyramids (Figures 8A and 8B).
(G-I) Examination of repolarization phase of individual spikes, indicative changes in voltage-gated K^+ current.
(G) Maximum repolarizing slope.
(H) t_{peak} to t_{rth} duration.
(I) t_{dth} to t_{rth} duration (spike width at threshold level). The significantly slower repolarization and broader spike suggest a reduction in voltage-gated outward current, not responsible for the decreased tendency to fire (Figures 8A and 8B). n = 11 for untreated and 12 for TTX-treated cells. *, $p<0.05$. **, $p<0.005$, *t*-tests.
(J-O) Similar examination of spike features in dentate granule neurons. Pattern of possible changes qualitatively similar to that in CA3 neurons, although none of the individual alterations reached statistical significance [$p>0.1$, *t*-tests; if anything, maximal rate of rise of action potential was decreased by chronic inactivity, in the wrong direction to account for the increased excitability (Figures 8C and 8D)]. Thus, voltage-gated ionic currents that determine the shape of individual action potentials are not major determinants of the differences in how CA3 and dentate neurons respond to inactivity. In contrast, changes in resting potential in CA3 and dentate neurons (Figure 8E) could reflect mechanisms that govern the firing pattern in a regionally-specific way.
(J-M) n = 6 for untreated and 5 for TTX-treated cells.
(N-O) n = 6 for untreated and 4 for TTX-treated cells (One TTX-treated cell of which action potential did not repolarize below threshold was excluded).

REFERENCES FOR SUPPLEMENTAL FIGURES

Bean, B.P. (2007). The action potential in mammalian central neurons. Nat. Rev. Neurosci. *8*, 451-65.

Henze, D.A., Buzsáki, G. (2001) Action potential threshold of hippocampal pyramidal cells in vivo is increased by recent spiking activity. Neuroscience *105*, 121-30.